Journal of Materials Chemistry

Dynamic Article Links

Cite this: J. Mater. Chem., 2011, 21, 5156

www.rsc.org/materials

PAPER

Surface plasmon resonance biosensing based on target-responsive mobility switch of magnetic nanoparticles under magnetic fields

Kyung Sig Lee,[a] Mongryong Lee,[b] Kyung Min Byun*[c] and In Su Lee*[a]

Received 3rd November 2010, Accepted 24th January 2011
DOI: 10.1039/c0jm03770b

A novel surface plasmon resonance (SPR) detection technique based on the programmed assembly of superparamagnetic iron oxide nanoparticles (SPIONs) and the corresponding change in mobility under external magnetic fields was demonstrated. In this approach, SPIONs act as a magnetophoretic mobility switch undergoing aggregation only in the presence of target analytes. The aggregated SPIONs which were magnetically attracted to a metal film create a layer over the sensor surface with a refractive index contrast, resulting in a notable SPR angle change. The experimental results indicated that the concentrations of the reactants such as SA and the size of the SPIONs play important roles in achieving enhanced SPR sensing. As a result, this study illustrates the potential for sensitive and selective detection of target molecules without the requirement of immobilized receptors on the sensor surface.

1. Introduction

The surface plasmon resonance (SPR) technique has been widely used in many studies involving interactions between surface-immobilized biomolecules since it can sense reactions on a quantitative basis without complex prior purification and labeling processes.[1] Due to its sensitive and fast response to refractive index change on a sensor surface, the SPR technique can be employed to detect the adsorption of biomolecules occurring at a thin metal film.[2] Over the past two decades, researchers have performed numerous SPR-based biomolecular interaction analyses to measure the biomaterial concentration, thickness, and binding kinetic data for specific biological analytes including antigen/antibody, ligand/receptor, protein/protein reactions, and DNA hybridizations.[3–9]

However, in practical SPR sensing applications, it is often difficult to directly detect biomolecules, especially those with low molecular weights, because of minute and nonspecific changes in refractive index.[10,11] In order to surmount these restrictions on sensitivity and selectivity, various enhanced SPR detection methods have been introduced.[12–16] For example, alternative methods of amplifying SPR signals have been developed by augmenting target molecules with colloidal Au nanoparticles.[17–19] Though many other interesting studies have focused on modifying a metal film with capturing ligands to promote the selective accumulation of target molecules,[20,21] several difficulties have been encountered in optimizing the ligand immobilization for efficient SPR measurements. Moreover, additional reactive layers or complex surface modifications may also be required depending on the target species.

Therefore, this study was intended to demonstrate the possibility of detecting target molecules without a ligand immobilization procedure. For this purpose, we used superparamagnetic iron oxide nanoparticles (SPIONs) which can provide different magnetic performances depending on whether they are in a dispersed or aggregated state.[22–24] SPIONs with a small size and large surface area have many superior properties such as good dispersability, a fast and effective binding process, and reversible and controllable attraction and flocculation when used in the detection and separation of a low number of biomolecules.[25–27] Thus, they have been used intensively for highly sensitive and selective biosensing systems[28–32] including SPR sensor.[33–36]

For instance, Weissleder and Lee exploited magnetic nanosensors composed of magnetic nanoparticles that can be switched from a dispersed to an aggregated state, resulting in a concomitant change in T_2 relaxation time of water protons, as detected by magnetic resonance imaging.[37–39] Inspired by their approach, we hypothesized that SPIONs can act as a magnetophoretic mobility switch undergoing aggregation only in the presence of target analytes. The aggregated SPIONs attracted to a metal film by externally applied magnetic fields create a layer over the sensor surface with a refractive index contrast (Scheme 1). In this paper, we proposed a novel SPR detection technique based on the programmed assembly of SPIONs and the corresponding change in mobility under external magnetic fields. We experimentally demonstrated a substantial improvement in SPR response, allowing for selective detection of target molecules

[a]Department of Applied Chemistry, Kyung Hee University, Gyeonggi-do, 446-701, Korea. E-mail: insulee97@khu.ac.kr; Fax: +82-31-202-7337; Tel: +82-31-201-3823
[b]Department of Display Materials Engineering, Kyung Hee University, Gyeonggi-do, 446-701, Korea
[c]Department of Biomedical Engineering, Kyung Hee University, Gyeonggi-do, 446-701, Korea. E-mail: kmbyun@khu.ac.kr

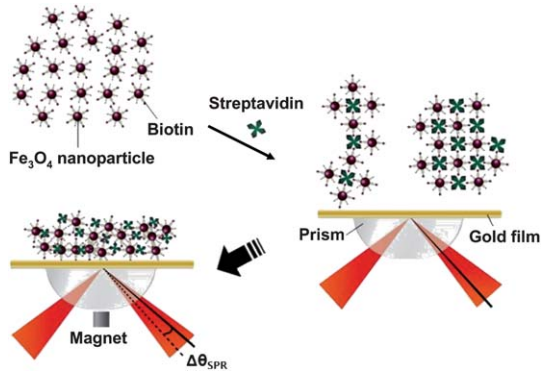

Scheme 1 SPR detection based on SPIONs and magnetic field.

without requiring immobilized receptors on the sensor surface. Moreover, the results of this study may contribute to make the SPR sensor chip reusable, which is critically advantageous in cases where the nanostructured SPR substrates for further enhancement in sensor performance require a high-cost of production.

2. Results and discussion

2.1 SPR characteristics of SPION-immobilized gold film

To verify the feasibility of SPIONs, SPR characteristics of a SPION-immobilized gold film were examined. A gold film with a thickness of 40 nm was evaporated onto an SF10 glass substrate after an evaporation of a 2 nm thick chromium adhesion layer and was then treated with an ethanol solution of 11-mercaptoundecanoic acid (MUA). The gold substrate was immersed into a chloroform suspension containing oleic acid stabilized SPION of various concentrations to assemble SPIONs on the surface *via* a self-assembled monolayer (SAM) of MUA, and then annealed at 400 °C to remove the underlying MUA. Scanning electron microscopy (SEM) analysis showed that the more number of SPIONs was immobilized on a gold film as with an increasing concentration of SPION suspensions from 0.5 to 2.0 Fe mg ml^{-1} (Fig. 1).

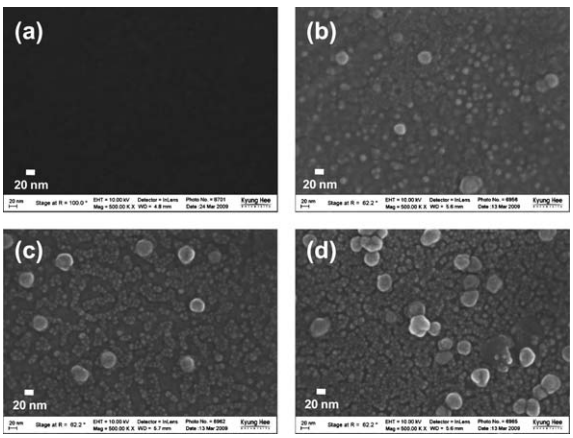

Fig. 1 SEM images of the gold films after treatment with SPION suspensions at (a) 0.0, (b) 0.5, (c) 1.0, and (d) 2.0 mg ml^{-1} concentration.

The SPR chip with immobilized SPIONs was loaded into an in-house optical setup. Our setup with a minimum measurable refractive index of $\Delta n \approx 5 \times 10^{-6}$ employed a polarized 10 mW He–Ne laser, a calibrated photodiode, and a motorized rotation stage with a nominal angular resolution of 0.002° pre-aligned for the sensor chip.[40] The detection limit of our SPR measurement system can be improved by employing a rotation stage with an enhanced angular resolution or by using a more powerful laser with a sensitive detector. The SPR measurements presented that the change in resonance angle increases significantly with the amount of SPIONs. The SPR angle for a gold film with no binding of SPIONs was 58.12° ± 0.07° and resonance shifts of 1.27°, 1.64°, and 2.85° were obtained for a gold film treated with SPION suspensions of 0.5, 1.0, and 2.0 Fe mg ml^{-1} concentrations, respectively (Fig. 2). Accordingly, it was confirmed that the use of SPIONs can provide additional weight for amplifying the SPR responses considerably.

2.2 Preparation of a colloidal suspension of biotin–SPIONs

In order to demonstrate our approach based on magnetophoretic mobility switch, SPIONs functionalized with biotin were employed to selectively recognize streptavidin (SA) proteins in the presence of magnetic fields. The SPIONs were prepared in advance by means of a previously reported procedure involving thermal decomposition of an iron–oleate complex.[41] The SPIONs were then modified with phospholipids with biotinylated poly(ethylene glycol) (biotin–PEG) tail groups, which can render a surface nonpolar.[42] After sequential processes of mixing the SPIONs and PEG–phospholipid and biotin–PEG–phospholipid in a $CHCl_3$ suspension, evaporating the solvent, and completely drying *in vacuo*, the surface was coated with a water-soluble and biocompatible shell which had little binding to nonspecific molecules and a high affinity for SA proteins. The addition of water followed by filtration of the floating matter produced a translucent colloidal suspension of SPIONs with biotin groups on their surfaces. The resulting biotin–SPIONs exhibited good colloidal stability in the aqueous suspension, as aggregation or phase separation was not observed even while applying a magnet. The numbers of biotin groups functionalized at the nanoparticle surfaces, as determined by inductively

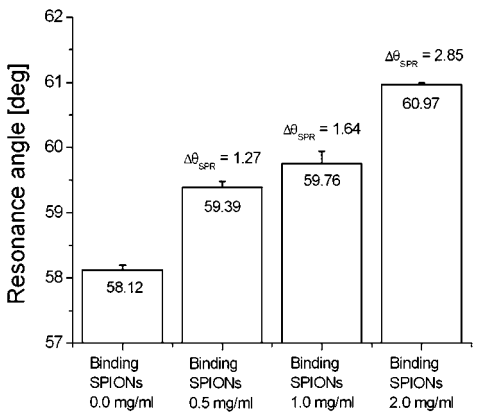

Fig. 2 Measurement of resonance angles after treatment with the SPION suspensions of concentrations at 0.0, 0.5, 1.0, and 2.0 mg ml^{-1}, respectively.

coupled plasma atomic emission spectroscopy (ICP AES), were 210, 150, and 56 for biotin–SPIONs for each nanoparticle with diameters of 12, 8, and 5 nm, respectively. When a small amount of SA was added to the suspension, the biotin–SPIONs were most likely assembled *via* an interaction between the SA and biotin, and the suspension became slightly cloudy. When a magnet was placed on the side of the vessel, the aggregates were readily attracted to the magnet and segregated from the suspension within several minutes (Fig. 3).

2.3 SPR response of biotin–SPION suspensions to target SA

Following the synthesis process, characterization of the mixture suspensions containing biotin–SPIONs and SA was performed using our SPR measurement setup. For magnetic attraction, a small neodymium permanent magnet was placed beneath a hemi-cylindrical prism. The intensity of magnetic fields at the sensor surface was measured to be 0.2 mT. Especially, note that wide surface areas with a diameter larger than 5 mm were illuminated to reduce measurement errors caused by uneven spatial distributions of the attracted aggregates. The optically averaged signals obtained may ensure the consistency and reliability of the SPR experiments.

Fig. 4 shows the SPR curves of 10 mM Fe suspension containing 12 nm sized biotin–SPIONs aggregated with 10 μM SA during a 20 min exposure to magnetic fields. For the first 5 min, the resonance angle shifted from 57.91° to 58.12° and the attraction process was almost complete after 10 min. A longer exposure for 40 min led to a slight increase in the resonance angle which became saturated at 58.19°. Thus, the overall resonance angle shift obtained was 0.28°. The results demonstrated that directional movement of the aggregates and the corresponding refractive index change resulted in a notable SPR angle shift when external magnetic fields sufficient to attract the aggregates toward the sensor surface were applied. On the other hand, when magnetic fields were not present, a stable and uniformly distributed suspension was maintained even for the aggregates, and a discernible SPR angle shift was not obtained. Further, from the control experiments using different targets of bovine serum albumin (BSA) instead of SA or using non-biotinylated SPIONs, the nanoparticles were in a well-dispersed state in the suspension as opposed to being transported to the sensor surface, supporting the hypothesis of a selective response of biotin–SPIONs to target SA molecules.

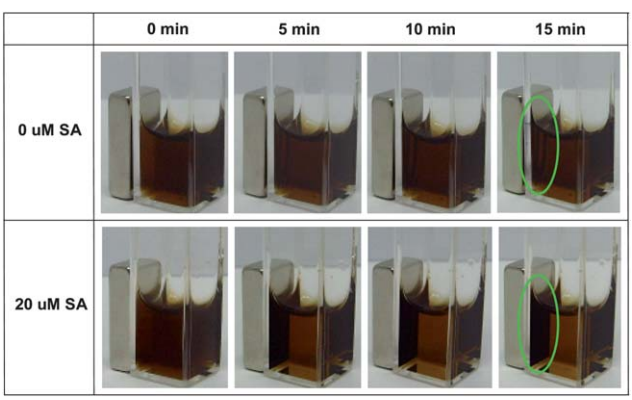

Fig. 3 Images demonstrating the aggregation and magnetic attraction of biotin–SPIONs upon the addition of a small amount of SA into the suspension.

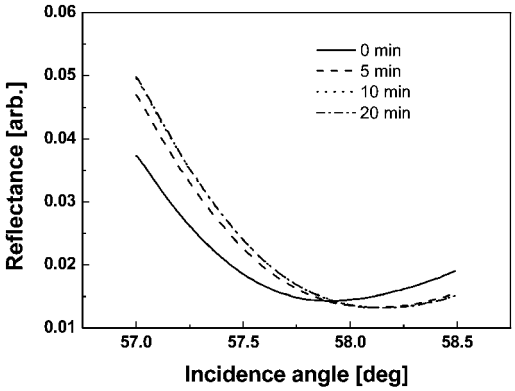

Fig. 4 SPR curves of 10 Fe mM suspension of 12 nm sized biotin–SPIONs aggregated with 10 μM SA during a 20 min exposure to magnetic fields.

2.4 Dependence of SPR response on reaction time and reactant concentration

Since the SPR technique is intrinsically surface sensitive, real-time kinetic data can be acquired to monitor the change in the refractive index on the sensor surface.[43–45] Time dependent resonance angles for magnetic attraction process are shown as a function of SA concentration in Fig. 5a. When the attraction was monitored at a low SA concentration of less than 2 μM, the

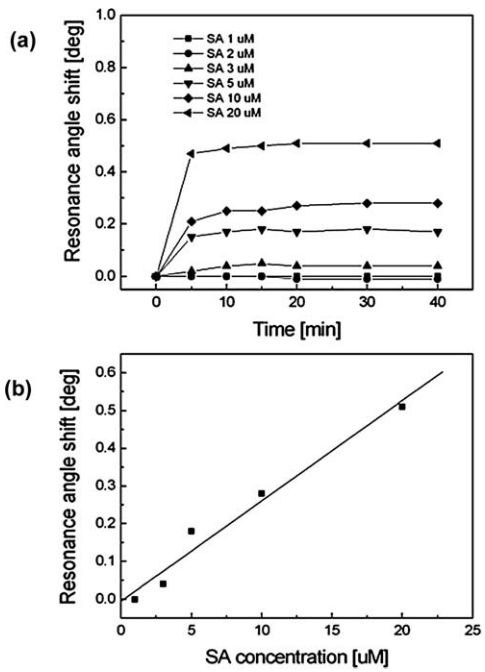

Fig. 5 Time courses of resonance angles for magnetic attraction process of the mixture suspension (a) containing 12 nm sized biotin–SPIONs of 10 Fe mM and SA of various concentration and (b) linear regression analyses between resonance angle shift and SA concentration.

resonance angle shift was insignificant due to the sparse aggregation of biotin–SPION, while SA concentrations larger than 5 μM produced a prominent SPR angle change of more than 0.15°. In general, the resonance angle increased rapidly at first until the reaction time reached 5 min, and then the response became nearly saturated as the time exceeded 20 min. The experimental data showed that the observed steady-state value of plasmon shift was strongly associated with the SA concentration. Using linear regression analysis, a relationship between SA concentration and resonance angle shift was determined (Fig. 5b). The correlation coefficient (R), where R denotes the degree of the linearity, was equal to 0.9850, implying a fairly linear sensing performance, with greater resonance angle shifts accompanying larger SA concentrations.

Fig. 6a illustrates the dependence of the SPR kinetics on the concentrations of reactants. Here, undiluted solution represents a mixture of 10 mM Fe containing biotin–SPIONs and 10 μM SA molecules. The time-dependent qualitative trends of the SPR angle were similar to the results in Fig. 6a, and an increase in resonance shift occurred as the aggregate solution became more concentrated. Interestingly, it was also found that aggregated SA molecules were measurable even at concentrations greatly diluted by more than 100 times, demonstrating that SPIONs can be useful for the detection of biomolecular samples at extremely low concentrations. It is also worth noting that no SPR shift was observed at very high SA concentrations, which can be explained by the Prozone effect where the presence of excessive target analytes saturate the binding sites of the nanoparticle probes and thus, hamper their aggregation.[46,47] For instance, when 10 μM of SA was added to the suspension of 0.25 mM Fe containing biotin–SPIONs, no resonance shift was observed (Fig. 6b).

2.5 Size effect of SPIONs on SPR detection

Further experiments were performed to examine the size effect of SPIONs. Fig. 7a shows size-dependent shifts in the plasmon angle for biotin–SPIONs with magnetic core diameters of 5, 8, and 12 nm where the concentrations of the target and Fe of the nanoparticles were held constant at 10 μM and 10 mM, respectively. Peak resonance shifts of 0.05°, 0.14°, and 0.28° were obtained for 5, 8, and 12 nm sized biotin–SPIONs. An important point to emphasize is that as the nanoparticles size increased, larger plasmon shifts occurred at constant Fe concentrations. Although the reason for this size dependency requires further investigation, it can be inferred that the increased resonance shifts for larger biotin–SPIONs were mainly due to the larger mass magnetizations and higher magnetophoretic mobilities.[48,49] In other words, since SA aggregates can be effectively attracted with larger SPIONs with a higher mobility at a given magnetic field strength, more aggregates are driven close to the sensor surface, transporting a higher mass and yielding a larger refractive index contrast. Fig. 7b shows the resonance angles obtained at various solution concentrations after exposure to magnetic fields for 40 min. As expected, more concentrated solutions and larger SPIONs resulted in more substantial shifts in the resonance angle. The data in Fig. 6 and 7 show that the reactant concentration and the size of the SPIONs play

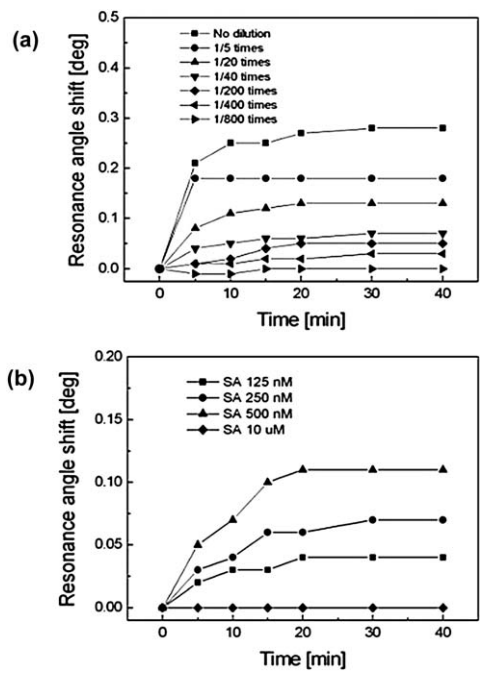

Fig. 6 Time courses of resonance angles for magnetic attraction process of (a) the suspensions diluted from the suspension of 10 Fe mM biotin–SPIONs of 12 nm size and 10 μM SA with various dilution ratio and (b) the suspension containing 12 nm sized biotin–SPIONs of 0.25 Fe mM and SA of various concentrations.

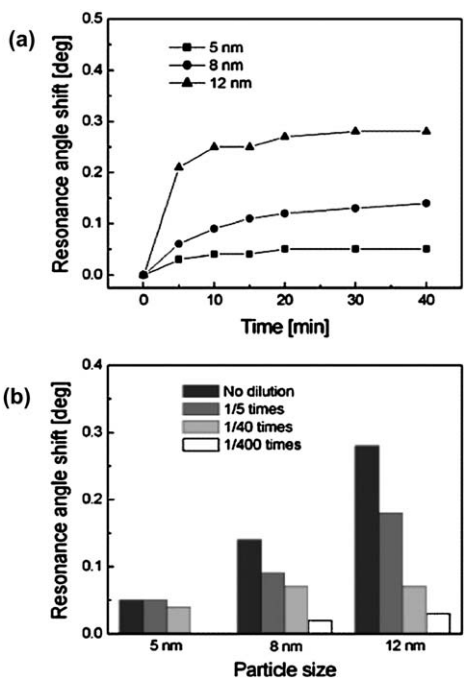

Fig. 7 (a) Time courses of resonance angles for magnetic attraction process of the mixture suspension of 10 μM of SA and 10 Fe mM of biotin–SPIONs with magnetic cores of 5, 8, and 12 nm diameter, respectively. (b) The resonance angles obtained from the suspensions diluted from the mixture suspension of 10 μM of SA and 10 Fe mM of biotin–SPION after an exposure to magnetic fields for 40 min.

important roles in achieving enhanced sensing performance of the SPR measurement.

2.6 Investigation of SA-responsive aggregation and magnetophoretic mobility switch of biotin–SPIONs

Finally, in order to validate the formation of SA aggregates and their attraction processes caused by biotin–SPIONs and external magnetic fields, optical and transmission electron microscopy (TEM) images were captured in various ways. Representative optical microscope images of 12 nm sized biotin–SPIONs bound with SA molecules are shown in Fig. 8a. 10 Fe mM biotin–SPIONs exposed to 0, 5, 10, and 20 μM SA solutions displayed vastly different degrees of aggregation. A higher SA concentration produced a larger number of aggregates with a detectable size. Transmission electron microscopy analysis of the same suspensions also evidenced the formation and size variation of the aggregates as a function of the SA concentration (Fig. 8b). Namely, higher SA concentrations tended to generate more complex structures with a large size, while no aggregation was observed in the target-free solutions. The other optical microscopy images in Fig. 9 show continuous and directional movements of the aggregates into a magnetic field. When the suspension was injected into a thin 40 μm gap between two glass windows and a magnet was placed to the right, the aggregates demonstrated collective transport to the right side, and bands composed of the attracted aggregates were created near the magnet within 15 min. At high SA concentrations, a more noticeable band structure was created due to the formation of large aggregates with strongly enhanced mobility. For the suspension without SA molecules, however, the biotin–SPIONs in a dispersed state remained uniformly distributed in the suspension, and no band structure associated with attracted aggregates was found. As a result, these observations qualitatively supported our investigation of the SPR characteristics of the biotin–SPION suspensions involving SA molecules under externally applied magnetic fields.

3. Experimental

3.1 Synthesis of biotin–SPION

General consideration. All reagents including $FeCl_3$ (Acros), sodium oleate (TCI), oleic acid, 1,2-distearoyl-*sn-glycero*-3-phosphoethanolamine-*N*-[methoxy(polyethylene glycol)-2000] (PEG-phospholipid, Avanti Polar Lipids, Inc.), 1,2-distearoyl-*sn-glycero*-3-phosphoethanolamine-*N*-[biotinyl(polyethylene glycol)-2000] (Biotin–PEG, Avanti Polar Lipids, Inc.), and streptavidin protein (SA, Thermo Scientific) were used as purchased without any purification. Analyses of transmission electron microscopy (TEM) were conducted with a JEOL JEM-2010. Scanning tunneling microscopy (SEM) was carried out with a LEO SUPRA 55 (Carl Zeiss, Germany). Inductively coupled plasma atomic emission spectroscopy (ICP AES) analyses were performed with a Direct Reading Echelle ICP (LEEMAN). Optical microscopy was carried out by using a BX51-75E21PO (Olympus). UV absorption and fluorescence were observed by using a V670 UV-Visible-NIR spectrophotometer (JASCO).

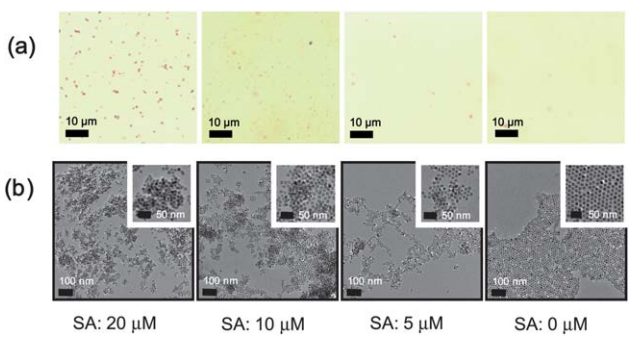

Fig. 8 (a) Optical microscopy and (b) TEM images of the suspensions containing 10 Fe mM Biotin–SPIONs and 0, 5, 10, and 20 μM SA, respectively.

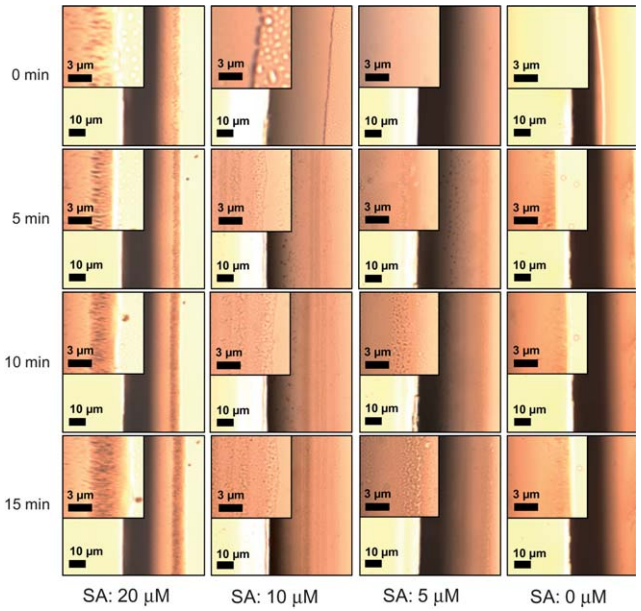

Fig. 9 Optical microscopy images taken by injecting the suspensions of 10 Fe mM Biotin–SPIONs and 0, 5, 10, and 20 μM SA, respectively, into a thin gap with 40 μm thickness between two glass windows and placing a magnet at the right sides.

Synthesis of biotin–SPION. Superparamagnetic iron oxide nanoparticles (SPIONs) stabilized by oleic acids were prepared through the previously reported procedure.[41] The purified SPIONs were dispersed in chloroform. The resulting SPIONs dispersed in chloroform were then encapsulated by Biotin–PEG–phospholipid shell. Typically, 0.25 ml of the organic dispersible SPIONs in $CHCl_3$ (40 mg ml^{-1}) was mixed with 2 ml of $CHCl_3$ solution containing a mixture of PEG–phospholipid (15 mg) and biotin–PEG–phospholipid (15 mg). After evaporating solvent, it was incubated at 80 °C in vacuum for 1 h. The addition of 5 ml water resulted in a clear and dark-brown suspension. After filtration, excess phospholipids were removed by ultracentrifugation, providing purified biotin–SPIONs. Non-biotinylated SPIONs for the control experiment were prepared through the identical coating procedure by using only PEG–phospholipid instead of the mixture of PEG–phospholipid and biotin–PEG–phospholipid.

3.2 Instrumentation for SPR experiments

Instrumentation for SPR experiments. We used a custom-made optical set-up to measure SPR signals, as shown in Fig. 10. The set-up was based on a concentric motorized rotation stage (URS75BCC, Newport) for angle scanning measurement with a nominal angular resolution at 0.002°. TM-polarized light was incident when a beam from 10 mW He–Ne laser ($\lambda = 632.8$ nm, 05-LHP-991, Melles Griot) passed through an optical polarizer and a beam collimator. The reflected light intensity was measured with a calibrated photodiode (1931-C, Newport). The minimum detectable refractive index of the setup was estimated to be $\Delta n \approx 5 \times 10^{-6}$ without any enhancement. For the preparation of SPR sensor chip, a gold film with thickness of 40 nm was first evaporated on a 20 × 20 × 0.5 mm thick SF10 slide glass substrate after an evaporation of a 2 nm thick chromium adhesion layer. The gold surface was cleaned sequentially in acetone and 70% ethanol solution for 10 minutes in a sonication bath. The chip was then rinsed with deionized distilled water and dried by blowing nitrogen. Finally, SPR sensor chip was index-matched to a SF10 hemi-cylindrical prism. A neodymium permanent magnet was placed beneath the prism and the intensity of magnetic fields was measured to be 0.2 mT at the sensor surface.

SPR examination of SPIONs immobilized on a gold film. A thin gold film with a thickness of 40 nm was evaporated on an SF10 glass substrate after an evaporation of a 2 nm thick chromium adhesion layer. After several repetitions of washing with ethanol and drying, SPR sensor chip was immersed in an ethanol solution (10 ml) containing 128 mg of 11-mercaptoundecanoic acid (MUA) and 0.1 ml of trifluoroacetic acid and gently shaken for 2 h, generating a self-assembled monolayer of MUA on the gold film. The resulting chip was washed with ethanol several times and completely dried *in vacuo*. The chip having MUA assembled gold film was immersed into a 2 ml of chloroform suspension containing SPIONs of 0.5, 1.0, and 2.0 mg ml^{-1} concentration, respectively, for 2 h, washed with hexane several time, and dried in air. The chip was then heated up 5 °C min^{-1} heating rate in a furnace and annealed in air condition for 5 h at 400 °C to remove 11-mercaptoundecanoic acid. The immobilization of SPIONs on a gold film was confirmed by the SEM analysis. Using a SPR measurement system, SPR characteristics were obtained for 0.0 to 2.0 mg ml^{-1} concentration of SPIONs immobilized on a gold film *via* a MUA SAM layer. Multiple (typically five) sites in a given sample were measured by translating the sample spatially to ensure consistency and thereby to reduce the standard error variation.

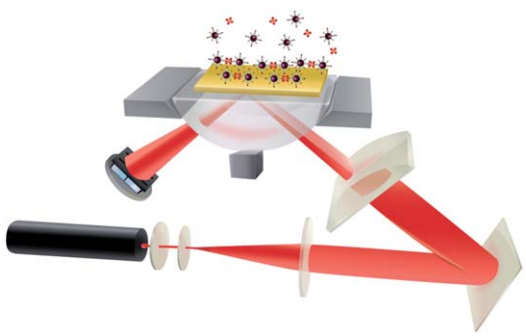

Fig. 10 Schematics of the optical measurement set-up and the SPR sensor chip.

SPR examination of mixture suspensions containing biotin–SPIONs and SA. For a suspension with a different dilution ratio varied from 40 (*i.e.*, an Fe concentration of 0.25 mg ml^{-1}) to 400 (*i.e.*, an Fe concentration of 0.025 mg ml^{-1}), SPR angles were measured with time as a function of SA concentration using an optical set-up.

4. Conclusions

In this study, we presented a novel methodology for SPR biosensor employing SPIONs as a mobility switch which undergoes target-responsive aggregation and attraction in the presence of external magnetic fields. We demonstrated that this newly developed method can provide a substantial improvement in the SPR response without ligand immobilization on the sensor surface. In addition, the sensing performance can be modulated by varying the concentrations of the reactants and the sizes of the SPIONs. It is expected that our SPION-based approach with good circulating properties can be easily adapted for a portable SPR sensor combined with a microfluidic system.[50] Our research toward this direction is currently underway.

Acknowledgements

This work was supported by a Korea Research Foundation Grant funded by the Korean Government (MOEHRD) (KRF-2008-314-C00192) (I.S.L). Kyung Min Byun thanks the support by Korea Science and Engineering Foundation (KOSEF) grant funded by the Korean government (MEST) (2009-0069267).

References

1 J. Homola, S. S. Yee and G. Gauglitz, *Sens. Actuators, B*, 1999, **54**, 3.
2 H. Raether, *Surface Plasmons on Smooth and Rough Surfaces and on Gratings*, Springer-Verlag, Berlin, Heidelberg, 1988.
3 X. Cui, R. Pei, Z. Wang, F. Yang, Y. Ma, S. Dong and X. Yang, *Biosens. Bioelectron.*, 2003, **18**, 59.
4 H. J. Watts, D. Yeung and H. Parkes, *Anal. Chem.*, 1995, **67**, 4283.
5 M. Malmqvist, *Curr. Opin. Immunol.*, 1993, **5**, 282.
6 B. P. Nelson, T. E. Grimsrud, M. R. Liles, R. M. Goodman and R. M. Corn, *Anal. Chem.*, 2001, **73**, 1.
7 H. J. Lee, D. Nedelkov and R. M. Corn, *Anal. Chem.*, 2006, **78**, 6504.
8 R. J. Leatherbarrow and P. R. Edwards, *Curr. Opin. Chem. Biol.*, 1999, **3**, 544.
9 B. Liedberg, C. Nylander and I. Lundstrom, *Biosens. Bioelectron.*, 1995, **10**, 1.
10 W. P. Hu, S.-J. Chen, K.-T. Huang, J. H. Hsu, W. Y. Chen, G. L. Chang and K.-A. Lai, *Biosens. Bioelectron.*, 2004, **19**, 1465.
11 Y. Xinglong, W. Dingxin, W. Xing, D. Xiang, L. Wei and Z. Xinsheng, *Sens. Actuators, B*, 2005, **108**, 765.
12 B. Sepúlveda, A. Calle, L. M. Lechuga and G. Armelles, *Opt. Lett.*, 2006, **31**, 1085.
13 K. M. Byun, S. J. Kim and D. Kim, *Opt. Express*, 2005, **13**, 3737.
14 L. Malic, B. Cui, T. Veres and M. Tabrizian, *Opt. Lett.*, 2007, **32**, 3092.
15 X. D. Hoa, A. G. Kirk and M. Tabrizian, *Biosens. Bioelectron.*, 2009, **24**, 3043.
16 P. P. Markowicz, W. C. Law, A. Baev, P. N. Prasad, S. Patskovsky and A. Kabashin, *Opt. Express*, 2007, **15**, 1745.
17 L. A. Lyon, M. D. Musick and M. J. Natan, *Anal. Chem.*, 1998, **70**, 5177.

18 L. He, M. D. Musick, S. R. Nicewarner, F. G. Salinas, S. J. Benkovic, M. J. Natan and C. D. Keating, *J. Am. Chem. Soc.*, 2000, **122**, 9071.
19 L. A. Lyon, D. J. Pena and M. J. Natan, *J. Phys. Chem. B*, 1999, **103**, 5826.
20 R. G. Nuzzo and D. L. Allara, *J. Am. Chem. Soc.*, 1983, **105**, 4481.
21 B. Johnsson, S. Löfås and G. Lindquist, *Anal. Biochem.*, 1991, **198**, 268.
22 N. Pamme and A. Manz, *Anal. Chem.*, 2004, **76**, 7250.
23 J. J. Lai, J. M. Hoffman, M. Ebara, A. S. Hoffman, C. Estournes, A. Wattiaux and P. S. Stayton, *Langmuir*, 2007, **23**, 7385.
24 M. Iijima, Y. Mikami, T. Yoshioka, S. Kim, H. Kamiya and K. Chiba, *Langmuir*, 2009, **25**, 11043.
25 Q. A. Pankhurst, J. Connolly, S. K. Jones and J. Dobson, *J. Phys. D: Appl. Phys.*, 2003, **36**, R167.
26 S. Mornet, S. Vasseur, F. Grasset and E. Duguet, *J. Mater. Chem.*, 2004, **14**, 2161.
27 H. Gu, K. Xu, C. Xu and B. Xu, *Chem. Commun.*, 2006, 941.
28 J.-M. Nam, C. S. Thaxton and C. A. Mirkin, *Science*, 2003, **301**, 1884.
29 Y. Weizmann, F. Patolsky, O. Lioubashevski and I. Willner, *J. Am. Chem. Soc.*, 2004, **126**, 1073.
30 X. L. Su and Y. Li, *Anal. Chem.*, 2004, **76**, 4806.
31 J. H. Gao, L. Li, P. L. Ho, G. C. Mak, H. W. Gu and B. Xu, *Adv. Mater.*, 2006, **18**, 3145.
32 B. Srinivasan, Y. Li, Y. Jing, Y. Xu, X. Yao, C. Xing and J.-P. Wang, *Angew. Chem., Int. Ed.*, 2009, **48**, 2764.
33 J. Wang, A. Munir, Z. Zhu and H. S. Zhou, *Anal. Chem.*, 2010, **82**, 6782.
34 S. D. Soelberg, R. C. Stevens, A. P. Limaye and C. E. Furlong, *Anal. Chem.*, 2009, **81**, 2357.
35 Y. Sun, D. Song, Y. Bai, L. Wang, Y. Tian and H. Zhang, *Anal. Chim. Acta*, 2008, **624**, 294.
36 Y. Teramura, Y. Arima and H. Iwata, *Anal. Biochem.*, 2006, **357**, 208.
37 J. M. Perez, L. Josephson, T. O'Loughlin, D. Högemann and R. Weissleder, *Nat. Biotechnol.*, 2002, **20**, 816.
38 J. M. Perez, L. Josephson and R. Weissleder, *ChemBioChem*, 2004, **5**, 261.
39 C. Kaittanis, S. A. Naser and J. M. Perez, *Nano Lett.*, 2007, **7**, 380.
40 K. M. Byun, S. J. Yoon, D. Kim and S. J. Kim, *Opt. Lett.*, 2007, **32**, 1902.
41 J. Park, K. An, Y. Hwang, J.-G. Park, H.-J. Noh, J.-Y. Kim, J.-H. Park, N.-M. Hwang and T. Hyeon, *Nat. Mater.*, 2004, **3**, 891.
42 B. Dubertret, P. Skourides, D. J. Norris, V. Noireaux, A. H. Brivanlou and A. Libchaber, *Science*, 2002, **298**, 1759.
43 L. Choulier, N. Rauffer-Bruyere, M. B. Khalifa, F. Martin, T. Vernet and D. Altschuh, *Biochemistry*, 1999, **38**, 3530.
44 P. Pfeifer, U. Aldinger, G. Schwotzer, S. Diekmann and P. Steinrucke, *Sens. Actuators, B*, 1999, **54**, 166.
45 M. A. Cooper and D. H. Williams, *Anal. Biochem.*, 1999, **276**, 36.
46 G. Y. Kim, L. Josepson, R. Langer and M. J. Cima, *Bioconjugate Chem.*, 2007, **18**, 2024.
47 I. Koh, R. Weissleder and L. Josephson, *Anal. Chem.*, 2009, **81**, 3618.
48 A. H. Latham, R. S. Freitas, P. Schiffer and M. E. Williams, *Anal. Chem.*, 2005, **77**, 5055.
49 Y. Jun, Y.-M. Huh, J.-s. Choi, J.-H. Lee, H.-T. Song, S. J. Kim, S. Yoon, K.-S. Kim, J.-S. Shin, J.-S. Suh and J. Cheon, *J. Am. Chem. Soc.*, 2005, **127**, 5732.
50 A. H. Latham and M. E. Williams, *Anal. Chem.*, 2008, **41**, 411.

